Article

JOURNAL OF
biomaterials
applications

Journal of Biomaterials Applications
0(0) 1–9

DOI: 10.1177/0885328215585682
jba.sagepub.com

SAGE

Analytical investigation of bilayer lipid biosensor based on graphene

Elnaz Akbari[1], Zolkafle Buntat[1], Elmira Shahraki[2], Ramtin Parvaz[3] and Mohammad Javad Kiani[4]

Abstract

Graphene is another allotrope of carbon with two-dimensional monolayer honeycomb. Owing to its special characteristics including electrical, physical and optical properties, graphene is known as a more suitable candidate compared to other materials to be used in the sensor application. It is possible, moreover, to use biosensor by using electrolyte-gated field effect transistor based on graphene (GFET) to identify the alterations in charged lipid membrane properties. The current article aims to show how thickness and charges of a membrane electric can result in a monolayer graphene-based GFET while the emphasis is on the conductance variation. It is proposed that the thickness and electric charge of the lipid bilayer (L_{LP} and Q_{LP}) are functions of carrier density, and to find the equation relating these suitable control parameters are introduced. Artificial neural network algorithm as well as support vector regression has also been incorporated to obtain other models for conductance characteristic. The results comparison between analytical models, artificial neural network and support vector regression with the experimental data extracted from previous work show an acceptable agreement.

Keywords

Monolayer graphene, lipid bilayer, conductance, artificial neural network, support vector regression, GFET

Introduction

Carbon-based material has been explored extensively to accommodate the advancing technology nowadays.[1–3] A single-layer graphene is sp^2-bonded carbon atoms arranged in the form of hexagonal lattice (honeycomb lattice) in a two-dimensional (2D) structure[4] comprising a thin layer of single carbon atoms. Comparing with most conventional materials, graphene exhibits unique electronic properties and it has become an extremely attractive material for use in future nanoelectronic devices particularly in sensor applications.[5,6] Among the many great properties of graphene are its remarkably high stiffness with Young's modulus of approximately 1000 GPa, its outstanding heat conductivity of $3000\,W\,(m\,K)^{-1}$, its high-speed electron mobility of $200{,}000\,cm^2\,(V\,s)^{-1}$ at room temperature and high specific surface area of $2600\,m^2\,g^{-1}$.[7–10] Therefore, graphene would represent a new revolutionary asset in material science, nanoelectronics and matter physics.[11]

Moreover, compared to any metal used on biosensors such as biomimetic membrane-coated types, graphene allows current to pass through it in a much more precise and effective manner and at higher speed. In many plant and animal cells, there is a two-layer covering called phospholipid bilayer surrounding the cell. Figure 1 depicts phospholipids, the molecules which form phospholipid bilayer.[12] These molecules can organize themselves by forming a pair of layers which form a covering that only some specific types of substances are merely able to infiltrate. Such a structure provides a barrier preventing unwanted materials from entering the cell.[13]

[1]Institute of High Voltage and High Current, Faculty of Electrical Engineering, Universiti Teknologi Malaysia, Johor Bahru, Malaysia
[2]Department of Communications Engineering, University of Sistan and Baluchestan, Zahedan, Iran
[3]Department of Electrical Engineering, Neyriz Branch, Islamic Azad University, Neyriz, Iran
[4]Department of Electrical Engineering, Islamic Azad University, Yasooj, Iran

Corresponding author:
Zolkafle Buntat, Institute of High Voltage and High Current, Faculty of Electrical Engineering, Universiti Teknologi Malaysia, Johor Bahru 81310, Malaysia.
Email: zolkafle@fke.utm.my

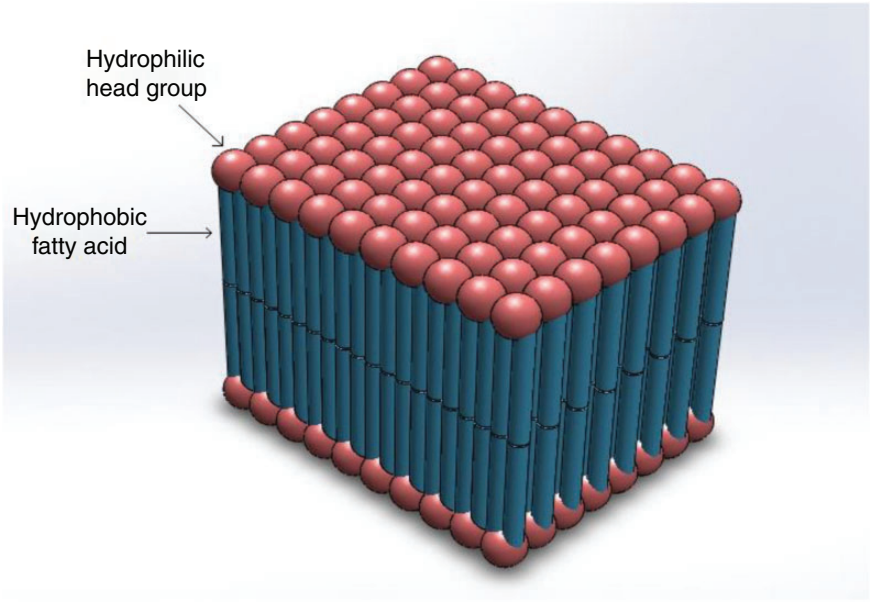

Figure 1. Structure of phospholipid bilayer.

There are two ends in each phospholipid: one end attracts water showing a hydrophilic behaviour, and the other end that acts in an opposite hydrophobic manner resisting water.[14,15] Normally there is water both outside and inside the cells, hence the molecules form themselves between two sheets, with the hydrophobic ends of both layers in inward direction and the hydrophilic ends of them pointing outwards.[16–18]

A key role of phospholipid bilayer is to prepare the structure to a cell. This is achieved when the hydrophobic and hydrophilic ends of phospholipids are naturally arranged, and when stable, cholesterol and sterols contribute to this too. Controlling the types of material that attach to or enter the cell through different ways by utilizing proteins is another function of phospholipid bilayer.[19] In order to distinguish the cell or to provide a space for some substances to attach to the membrane, the types of the protein which develop from the top of membrane can be utilized. Moreover, certain kinds of protein are able to form channels or tunnels to let some materials enter. A number of channels are open towards some kinds of molecules all the time, but some channels cannot close or open without providing the required energy. Since such type of transport performs in both ways, that is the materials can both enter and exit the cell, it is called active transportation. This transportation is usually used with substances such as sodium, potassium and calcium. The electronic properties of graphene are accepted by an altered lipid bilayer which adsorbs on the surface.[20] In order to observe and check the electrical conditions of biorecognition occurrence which cause alterations in the perpendicularity of the membrane, one can utilize a biomimetic lipid membrane on grapheme-based electrolyte-gated transistor. The bacterial motion of antimicrobial peptides can be electrically detected by graphene according to a multi-part interaction of a biomolecular doping and ionic screening influence.[21] The signs of lipid charges together with the transference perceived in the Dirac point show that the lipid membranes created a charge-impurity potential. These signs also depict that the current membranes of lipid modify and accept the electronic properties of graphene to a great extent. Suppose that the current lipids are equally divided into two leaflets, the degree of charged pollutants concentrated in the membranes of lipid is estimated by the distance between the surface area and a lipid head group because of graphene's electrically neutral properties.[22] The conductance of graphene might be modified and simulated through the adsorption of charged lipid bilayer on the surface of the membrane. In terms of electrical area, it is possible to utilize electrolyte-gated biomimetic membrane-graphene biosensor for practicing biorecognition that leads to some alterations in the membrane unity and entirety.[23] In the present research, the influence of Q_{LP} and L_{LP} on the conductance of graphene-based FET has been assessed.

Proposed model

We begin the modelling by carrier concentration given as

$$n = \int D(E) f(E) d(E) \tag{1}$$

where $f(E)$ is Fermi Dirac distribution and $D(E)$ shows density of state and can be written as[24]

$$D(E) = \frac{1}{3\pi t a_{c-c}} \frac{E}{\sqrt{E^2 - \left(\frac{E_g}{2}\right)^2}} \quad (2)$$

In which $a_{C-C} = 1.42\text{Å}$ represents carbon–carbon (C–C) bond length, and $t = 2.7(eV)$ is the nearest neighbour C–C tight binding overlap energy. E_g is the band gap energy which can be written for monolayer graphene as[24,26]

$$E_g = 2\pi\sqrt{3}\left(\frac{p}{N+1} - \frac{2}{3}\right) \quad (3)$$

in which p signifies an integer number, and the Fermi Dirac probability function $f(E)$ is defined as[27]

$$f(E) = \frac{1}{\exp\left(\frac{E-E_F}{k_B T}\right) + 1} \quad (4)$$

where E_F is Fermi energy , K_B is Boltzmann's constant, T is temperature and E is energy then the *E. coli* concentration is written as

$$n = \int \frac{1}{3\pi t a_{c-c}} \frac{E}{\sqrt{E^2 - \left(\frac{E_g}{2}\right)^2}} \cdot \frac{1}{\exp\left(\frac{E-E_F}{k_B T}\right) + 1} .d(E) \quad (5)$$

The quantum capacitance is shown as[28]

$$C_q = \frac{\delta Q}{\delta V} \quad (6)$$

In which Q is the charge measured in coulombs and $\delta Q = e.\delta n_{Total}$, e is electron charge, $n_{Total} = n + n'$, where n is inherent carrier concentration and n' is the amount of carrier concentration when lipid is injected.

$\partial V = \frac{\partial E}{e}$ is the voltage applied to the device and C_q is given as[29]

$$C_q = \frac{e\partial n_{Total}}{\frac{\partial E}{e}} \quad (7)$$

which becomes by a simple mathematical rearrangement

$$C_q = e^2 \frac{\partial n_{Total}}{\partial E} \quad (8)$$

Using the definition of n_{Total}, the following equation can be written for quantum capacitance

$$C_q = e^2 \frac{\partial n}{\partial E} + e^2 \frac{\partial n'}{\partial E} \quad (9)$$

Figure 2 depicts graphene electrolyte-gated FET device.

The factors on which the conductance of the GFET channel relies consist of the biomimetic membranes of diverse surface charges which always concentrate on the charged lipid bilayer and graphene, adsorbed by the graphene as well as graphene organization and the source–drain voltage. When the density of charge carrier changes in the channel, it imposes some effects on the graphene-based FET conductance.[30] Figure 3 depicts the alterations in the conductance of the channel as a result of the thinning effect of the membrane.

The alterations in the thickness of membrane and its electric charge lead to the absorption of several ions. On the other hand, the conductance of the biosensor based on graphene has been transformed by the solution. These two, in turn, cause the ions inside the

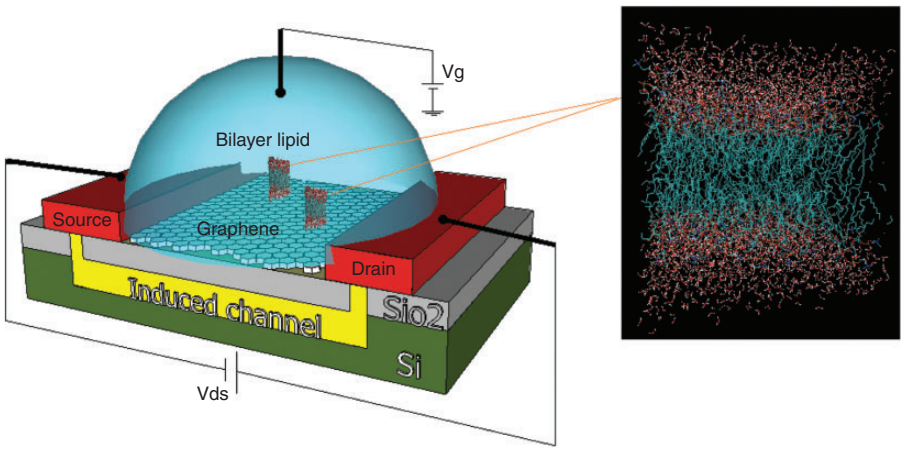

Figure 2. Schematics of electrolyte-gated FET based on graphene as biosensor.

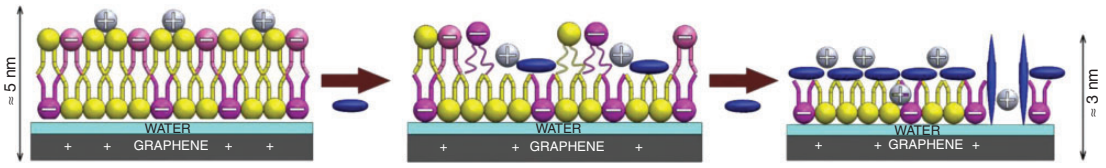

Figure 3. Lipid bilayer adsorption by using single-layer graphene.

solution to be attracted by the sensor. Conductance can be a function of thickness and charge of bilayer lipid, in the biosensor based on biomimetic membrane-coated graphene.[31] The current study aims to propose a novel model for GFET through which the alterations in thickness and electric charge can be predictable. That is, the model should be able to simulate the GFET conductance dependent on thickness, electric charge and propose parameters for them. Therefore, FET modelling is used to perceive the function and effect of lipid bilayer more comprehensively.[32] Through this modelling, in fact, an equation can be gained which explains the conductance, electric charge (Q_{LP}) and thickness (LL_P) well.

The L_{LP} and Q_{LP} should be considered as the following to confirm the suggested model

$$n' = \delta Q_{LP} + \psi L_{LP} \tag{10}$$

where (δ) and (ψ) are the electric charge and thickness parameter, respectively. As a result, the quantum capacitance can be written as

$$C_q = e^2.\frac{1}{3\pi t a_{c-c}}\frac{E}{\sqrt{E^2-\left(\frac{E_g}{2}\right)^2}}.\frac{1}{\exp\left(\frac{E-E_F}{k_BT}\right)+1} + e^2\delta\frac{Q_{LP}}{\partial t}\frac{\partial t}{\partial E} + e^2\psi\frac{\partial L_{LP}}{\partial t}\frac{\partial t}{\partial E} \tag{11}$$

The GFET conductance can be shown as follows

$$G = \left(e^2.\frac{1}{3\pi t a_{c-c}}\frac{E}{\sqrt{E^2-\left(\frac{E_g}{2}\right)^2}}.\frac{1}{\exp\left(\frac{E-E_F}{k_BT}\right)+1} + e^2\delta\frac{\partial Q_{LP}}{\partial t}\frac{\partial t}{\partial E} + e^2\psi\frac{\partial L_{LP}}{\partial t}\frac{\partial t}{\partial E}\right).V_{ds}.\mu_e \tag{12}$$

Corresponding with the extracted data[33] which is revealed in Table 1, the GFET conductance model proposed in this paper has membrane thicknesses and lipid bilayers charged differently, which are depicted as parameter ψ for L_{LP} and δ for Q_{LP}.

Based on the presented conductance model and also according to the iteration method, the following control parameter can be proposed

$$\delta = 27.34Ln(Q_{LP}) + 18.254 \tag{13}$$

According to the analytical model, the lipid bilayers charged will improve by increasing the amount of lipid concentration. As shown in Equation 13, parameters $a = 27.34$ and $b = 18.254$ are calculated.

Furthermore, thickness is another controlling parameter that is shown by ψ and has influence on the rate of conductivity. As demonstrated in the following equation, c and d are two constant parameters obtained from the extracted data

$$\psi = -0.416\mathrm{Ln}(L_{LP}) + 0.7192 \tag{14}$$

In the same method as before, c and d are calculated as: $c = -0.416$ and $d = 0.7192$.

In order to prove that membrane thickness of the lipid bilayer and the electric charge which charged the graphene-based biosensor change, in the present paper, the experimental data have been revealed together with the model that suggested the structure of electrolyte-gated FET based on graphene. According to the discussion earlier, it can be said that because of electronic instruments on the p-doping and n-doping materials, a remarkable alteration happens in $V_{g.min}$ of the ambipolar FET showing reaction to the electric charged lipid membranes alteration and changes of biomimetic membranes thickness.

Table 1. Control parameter values for Q_{LP} and L_{LP}

		δ	ψ
Q_{LP}	Neutral	0.13	–
	Negative	0.26	–
	Positive	−1.3	–
L_{LP}	10 nm	–	0.21
	100 nm	–	0.15
	1000 nm	–	0.07
	10,000 nm	–	0.05

Artificial neural network (ANN) and support vector regression (SVR) models

This study aims to carry out a comparative study between SVR[34,35] and back-propagation ANNs to assess their characteristics and potentials in the prediction of I–V characteristics. ANNs can be identified as a simplified mathematical model based on the neurological structure of human brain. The ability of ANN in determining complex relationships among variables makes this technique one of the most powerful tools for data modelling.[36]

Recently, SVR has been employed for prediction in chemical applications. SVR is another technique in computational intelligence associated with NN and is fundamentally based on the theory of statistical learning proposed by Vapnik.[37–39] In our research, we use the ε-SVR which gives an approximate function $f(x)$ which limits the deviations from the target y_i in the training data set (i.e.$\{(x_1,y_1)\ldots(x_I,y_L)\} \subseteq (X \times Y)^l$) not to exceed a maximum value ε and makes it as flat as possible.[40,41] In other words, errors are neglected as long as they are smaller than a pre-specified value ε. Unlike the ANN, training of the SVR includes convex optimization in which there are no local minima.[37] A transformation function Φ is applied in the SVR algorithm to the original points to transform them from the initial input space to a feature space F of a higher dimension. In the obtained new space, a linear model is constructed corresponding to a non-linear model in the original space. Consider a simple linear problem; for this case, the transformation function is in the form of $f(x) = <w,\Phi(x)> + b$ where $w \in X$, and $b \in \Re$. Here $<w,\Phi(x)>$ represents the dot product of the input patterns, x in the feature space.[38,40,42] As a matter of fact, the support vectors are the data points which are used in the description of the searched function.[43] In the presence of noise, working with a soft margin, obtained from the support vector machines would be more plausible. This can be evidently realized by slack variables $\xi_i^-,\xi_i^+ \geq 0$ with which the mathematical formulation can be extended in convex optimization[37]

$$\frac{1}{2}\|W\|^2 + C\sum_{i=1}^{l}(\xi_i^+ + \xi_i^-) \tag{15}$$

In order to ensure flatness, the equation above must be minimized by $\|W\|^2 = w,w$ and applying the constraints $(w.\phi(x_i)) + b - y_i = \varepsilon + \xi_i^- y_i - (w.\phi(x_i)) - b \leq \varepsilon + \xi_i^+$.[37,43] The constant C determines the trade-off between flatness and the amount of outliers of the ε-tube, which is handled in this study with the ε-intensive loss function[44]

$$|\xi|_\varepsilon = \begin{cases} 0 & if\ |\xi| \leq \varepsilon \\ |\xi| \leq \varepsilon & otherwise \end{cases} \tag{16}$$

Table 2. The selected values for ε, C and γ.

	ε	C	γ
Neutral	4	158.9400	0.05
Negative	3.8	144.7149	0.06
Positive	3	133.84	0.1
10 pm thickness	4.2	163.45	0.04
10,000 nm thickness	3.7	262.50	0.07

Employing the kernel function, one can derive a solution for the original regression problem, without the need to consider the transformation $\Phi(x)$ applied to the data explicitly. In this study, we have implemented radial basis functions (RBF). The accuracy of the model for the ε-SVR with RBF kernel function is dependent upon the parameters ε, C and γ. As previously mentioned, the accuracy of the approximated function is determined by the magnitude of epsilon. For values of epsilon larger than the range of target data, expecting accurate results is a little over-optimistic. One can expect over-fitting for zero epsilon. Thus, epsilon must be chosen in a way that it somehow reflects the data. The values of insensitivity function ε and parameters C and γ were selected by trial and error method and tabulated in Table 2.

Results

Figure 4 shows that using the gate voltage to the biomimetic membrane, the ambipolar performance resulted from the conductance of GFET-based graphene was obvious. In order to estimate the lowest level of conductance of the graphene layer determined using transfer characteristic curve, the doping conditions of graphene are checked. On the whole, measurement and modulation of lipid bilayer are strongly demonstrated by $V_{g\min}$ shift (at the Dirac point). However, when such alteration is estimated from the location of the smallest level of conductivity in bare graphene, the degree of alterations in voltage from negative and positive lipids are similar. While some alterations are happening in the electric charges of biomimetic membrane-coated graphene biosensor, an alteration is observed in the conductivity graph too. Hence, the molecules which are electrically charged better would be absorbed and a bigger number of molecules are attracted to the sensor. It causes the total density to reduce following $V_{g\min}$

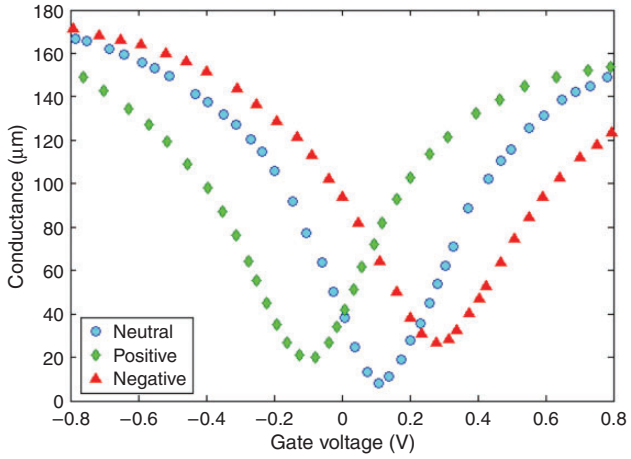

Figure 4. Conductance model comparison for neutral, positive and negative charged.

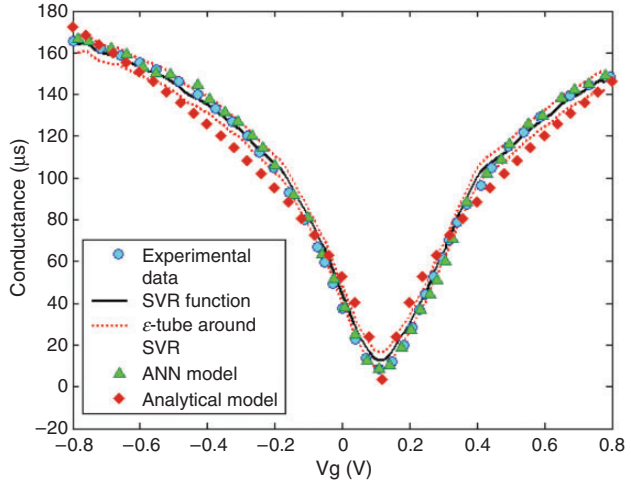

Figure 5. Comparison between bipolar transfer curves for neutral membrane.

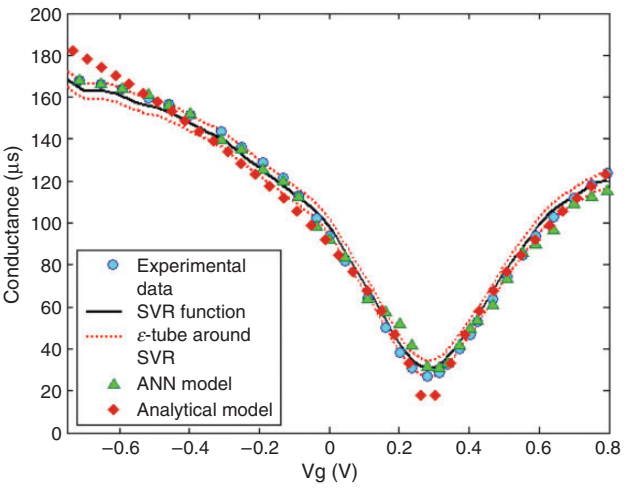

Figure 6. Comparison between bipolar transfer curves for negative membrane.

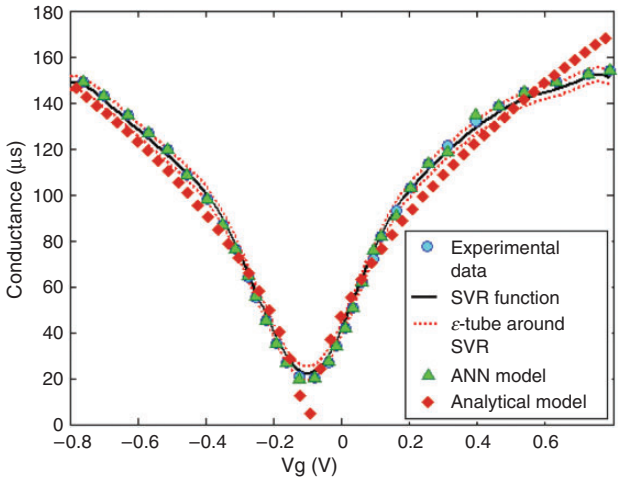

Figure 7. Comparison between bipolar transfer curves for positive membrane.

changes on the device. If the membrane is negative compared with that of exposed graphene, the positive change and conductivity in the Dirac point will increase very little.

As indicated in Figure 5, in order to estimate the transfer curve, before using electrolyte solution, pure water is used as a water gated in GFET structure. The empirical result obtained based on Ang et al.[33] and analytical SVR and ANN models of lipid bilayer-based biosensor remarkably corresponds.

Figures 6 and 7 show the bipolar transfer curves for negative and positive membrane, respectively.

The reason for this is due to the negative alterations in membrane that cause the remaining pollution charges to enhance. According to a measurable Dirac point shift, it would be possible to obtain a detection-charged lipid bilayer. Accordingly, the present research primarily aims to provide a novel model appropriate for biomimetic membrane-coated graphene biosensors. A function of gate voltage which is the type and thickness of coated charge, according to such model, is simulated and then the control parameters can be recommended. Afterwards, in order to determine the association of the liquid gate voltage and its conductance where the electrodes are drain and source contacts, GFET modelling is utilized so that a broader view related to the function of lipid bilayer and its thickness can be gained. The validation parameters for three different models are presented in Table 3.

Figure 8 depicts that if, on the graphene surface, the membrane becomes thicker, the $V_{g\min}$ should be left-shifted intensively. Hence, one can say that the sensitivity of $V_{g\min}$ to membrane thickness and electric

Table 3. Validation parameter for three models.

	Analytical			ANN			SVR		
	Neutral	Negative	Positive	Neutral	Negative	Positive	Neutral	Negative	Positive
MNS	0.0129	0.0051	0.0049	0.0015	0.0012	0.0002	0.0005	0.0010	0.0001
R2	0.9023	0.9669	0.9842	0.9905	0.9904	0.9987	0.9991	0.9922	0.9986
Q2	0.7775	0.9264	0.9260	0.9843	0.9865	0.9976	0.9935	0.9893	0.9985
RSS	0.2345	0.0853	0.0396	0.0377	0.0292	0.0043	0.0033	0.0250	0.0050
TSS	2.4007	2.5774	2.5104	3.9620	3.0480	3.4619	3.6430	3.1881	3.6648
SSE	0.4767	0.1639	0.1617	0.0578	0.0363	0.0072	0.0215	0.0312	0.0050
PRESS	0.5340	0.1898	0.1857	0.0620	0.0411	0.0082	0.0237	0.0341	0.0055

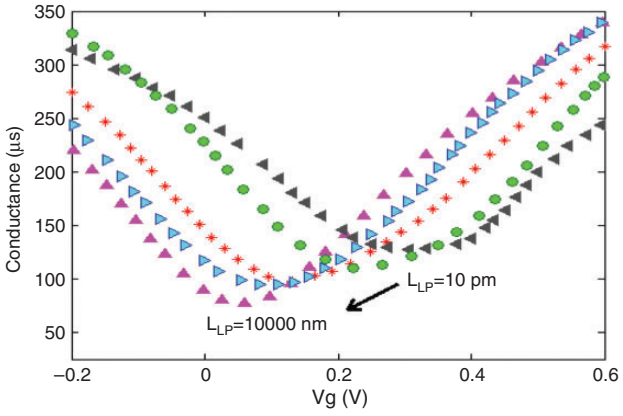

Figure 8. The effect of different membrane thickness on graphene biosensor.

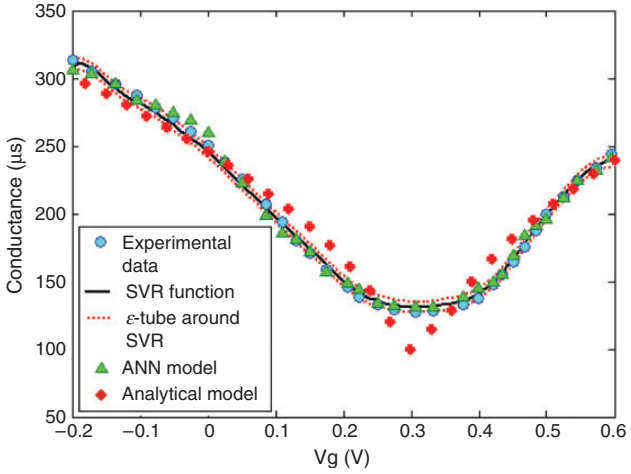

Figure 9. The membrane thickness = 10 pm.

charge is high. Since, in the presence of thick membrane, the graphene would be n-doped, the above finding is in agreement with the leftward gate voltage shift. It means that, according to Ang et al.,[33] when the

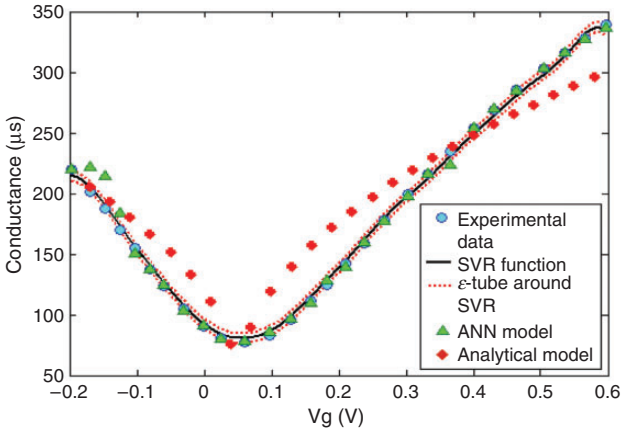

Figure 10. The membrane thickness = 10,000 nm.

membrane thickness changes from 0.01 nM to 10 µM, and becomes higher, the alteration can happen in a bigger range accordingly and $V_{g\min}$ would shift leftwards.

The Vg characteristic of graphene-based GFET with $L_{LP} = 10$ pm is shown in Figure 9. If Figures 9 and 10 are compared with each other, they will reveal that based on the proposed parameters (δ and ψ), the changes described by Ang et al.[33] are indicated similar by the biomimetic membrane-coated graphene biosensor model. Theoretical and experimental findings show that when the thickness of membrane becomes higher, an obvious shift will be observed in $V_{g\min}$.

In Figure 10, after the theoretical and experimental data were compared, it was depicted that 10 meV shift in $V_{g\min}$ resulted in a membrane as thick as 10,000 nm.

Conclusion

It is indicated that biosensors based on nanomaterials are powerful tools aimed at providing selective identification of biomedical diagnosis and biological systems (e.g., bacteria, virus). The current study provides a

function for the total graphene conductance associated with the adsorbed lipid bilayer thickness (L_{LP}) and the electric charge (Q_{LP}). Moreover, it was revealed that a reduction of lipid thickness and the alterations (from negative to positive) in the electrical charge in terms of the gate voltage ($Vg_{,min}$) cause a remarkable alteration in the smallest level of (minimum) conductance. Based on the experimental data, the difference of $Vg_{,\,min}$ current model has been employed as a platform for detection for which the sensor control parameters have been determined. The accuracy of the suggested model provided was approved by the experimental data. Besides, in order to forecast the performance of graphene in graphene-based biosensors, the utilization of δ and ψ (as the biosensor control parameters) is made easy. In addition to the analytical model, ANN and SVR models were also developed for the conductance characteristics of graphene-based biosensor with FET structure. This sensing principle based on ionic screening variation and the dynamics of membrane diffusion on graphene can be used in other systems such as gated control of ion channels and ligand receptor binding.

Funding

The authors would like to thank Ministry of Education (MOE), Malaysia (grant Vot. No. 4F382) and the Universiti Teknologi Malaysia (grant Vot. No. 07H56) for the financial support received during the investigation.

Declaration of conflicting interests

None declared.

References

1. Geim AK and Novoselov KS. The rise of graphene. *Nat Mater* 2007; 6: 183–191.
2. Geim AK. Graphene: status and prospects. *Science* 2009; 324: 1530–1534.
3. Akbari E, Arora VK, Enzevaee A, et al. Gas concentration effects on the sensing properties of bilayer graphene. *Plasmonics* 2014; 9: 987–992.
4. Rao CNR and Sood AK (eds). *Graphene: synthesis, properties, and phenomena*. John Wiley & Sons, 2013.
5. Anderson BA and Nowak EJ. Graphene-based transistor. U.S. Patent No. 7,732,859, 8 June 2010.
6. Akbari E, Buntat Z, Ahmad MH, et al. Analytical calculation of sensing parameters on carbon nanotube based gas sensors. *Sensors* 2014; 14: 5502–5515.
7. Novoselov K, Fal V, Colombo L, et al. A roadmap for graphene. *Nature* 2012; 490: 192–200.
8. Neto AC and Geim A. Graphene: graphene's properties. *New Scientist* 2012; 214: iv–v.
9. Neto AC, Guinea F, Peres N, et al. The electronic properties of graphene. *Rev Mod Phys* 2009; 81: 109.
10. Zhu Y, Murali S, Cai W, et al. Graphene and graphene oxide: synthesis, properties, and applications. *Adv Mater* 2010; 22: 3906–3924.
11. Amiri IS, Barati B, Sanati P, et al. Optical stretcher of biological cells using sub-nanometer optical tweezers generated by an add/drop microring resonator system. *Nanosci Nanotechnol Lett* 2014; 6: 111–117.
12. Edidin M. Lipids on the frontier: a century of cell-membrane bilayers. *Nat Rev Mol Cell Biol* 2003; 4: 414–418.
13. Dise CA, Goodman D and Rasmussen H. Definition of the pathway for membrane phospholipid fatty acid turnover in human erythrocytes. *J Lipid Res* 1980; 21: 292–300.
14. Rütters H, Sass H, Cypionka H, et al. Phospholipid analysis as a tool to study complex microbial communities in marine sediments. *J Microbiol Methods* 2002; 48: 149–160.
15. Alessio P, Pavinatto FJ, Oliveira Jr ON, et al. Detection of catechol using mixed Langmuir–Blodgett films of a phospholipid and phthalocyanines as voltammetric sensors. *Analyst* 2010; 135: 2591–2599.
16. Sada E, Katoh S, Terashima M, et al. Effects of solute hydrophobicity and phospholipid composition on permeability of composite membranes containing phospholipids. *Biotechnol Bioeng* 1986; 28: 1–6.
17. Kang SH, Lee HS, Lee J, et al. Nanoporous silicified phospholipids and application to controlled glycolic acid release. *Nanoscale Res Lett* 2008; 3: 355–360.
18. Leonenko Z, Cramb DT, Amrein M, et al. Atomic force microscopy: interaction forces measured in phospholipid monolayers, bilayers and cell membranes. *Applied scanning probe methods IX*. Berlin Heidelberg: Springer, 2008, pp.207–234.
19. Penno A, Hackenbroich G and Thiele C. Phospholipids and lipid droplets. *Biochim Biophys Acta Mol Cell Biol Lipids* 2013; 1831: 589–594.
20. Lei H, Zhou X, Wu H, et al. Morphology change and detachment of lipid bilayers from the mica substrate driven by graphene oxide sheets. *Langmuir* 2014; 30: 4678–4683.
21. Burke PJ. Charging the quantum capacitance of graphene with a single biological ion channel. *Biophys J* 2014; 106: 499a–500a.
22. Wang T, Zhu S and Jiang X. Toxicity mechanism of graphene oxide and nitrogen-doped graphene quantum dots in RBCs revealed by surface-enhanced infrared absorption spectroscopy. *Toxicol Res* 2015. DOI: 10.1039/C4TX00138A.
23. Kraszewski S, Bianco A, Tarek M, et al. Insertion of short amino-functionalized single-walled carbon nanotubes into phospholipid bilayer occurs by passive diffusion. *PLoS One* 2012; 7: e40703.
24. Lundstrom M and Guo J. *Nanoscale transistors: device physics, modeling and simulation*. Springer Science & Business Media, 2006.
25. Wong H-SP and Akinwande D. *Carbon nanotube and graphene device physics*. Cambridge University Press, 2010.
26. Ismail R, Ahmadi MT and Anwar S (eds). *Advanced nanoelectronics*. CRC Press, 2012.
27. Datta S. *Quantum transport: atom to transistor*. Cambridge University Press, 2005.
28. Xia J, Chen F, Li J, et al. Measurement of the quantum capacitance of graphene. *Nat Nanotechnol* 2009; 4: 505–509.

29. Shylau A, Kłos J and Zozoulenko I. Capacitance of graphene nanoribbons. *Phys Rev B* 2009; 80: 205–402.
30. Magliulo M, Mallardi A, Mulla MY, et al. Electrolyte-gated organic field-effect transistor sensors based on supported biotinylated phospholipid bilayer. *Adv Mater* 2013; 25: 2090–2094.
31. Mikucki M and Zhou Y. Electrostatic forces on charged surfaces of bilayer lipid membranes. *SIAM J Appl Math* 2014; 74: 1–21.
32. Wang YY, Pham TD, Zand K, et al. Charging the quantum capacitance of graphene with a single biological ion channel. *ACS Nano* 2014; 8: 4228–4238.
33. Ang PK, Jaiswal M, Lim CHYX, et al. A bioelectronic platform using a graphene−lipid bilayer interface. *ACS Nano* 2010; 4: 7387–7394.
34. Balabin RM and Lomakina EI. Support vector machine regression (LS-SVM)—an alternative to artificial neural networks (ANNs) for the analysis of quantum chemistry data? *Phys Chem Chem Phys* 2011; 13: 11710–11718.
35. Balabin RM, Safieva RZ and Lomakina EI. Wavelet neural network (WNN) approach for calibration model building based on gasoline near infrared (NIR) spectra. *Chemometr Intell Lab Syst* 2008; 93: 58–62.
36. Specht DF. A general regression neural network. *IEEE Trans Neural Netw* 1991; 2: 568–576.
37. Smola AJ and Schölkopf B. A tutorial on support vector regression. *Stat Comput* 2004; 14: 199–222.
38. Cristianini N and Shawe-Taylor J. *An introduction to support vector machines and other kernel-based learning methods* 2000; .
39. Anthony M. *Computational learning theory*. Cambridge University Press, 1997.
40. Stahlbock R and Lessmann S. *Potential von Support Vektor Maschinen im analytischen Customer Relationship Management*. Hamburg, Arbeitspapier: Universität Hamburg, 2004.
41. Welling M. *Support vector regression*. Toronto: Department of Computer Science, University of Toronto, 2004.
42. Schölkopf B, Burges CJ and Smola AJ (eds). *Advances in kernel methods: support vector learning*. MIT Press, 1999.
43. Gunn SR. *Support vector machines for classification and regression*. ISIS technical report, 1998, p.14.
44. Müller K-R, et al. Predicting time series with support vector machines. In: *Artificial neural networks—ICANN'97*. Berlin Heidelberg: Springer, 1997, pp.999–1004.